PHYSICAL REVIEW B **82**, 165445 (2010)

Imaging localized states in graphene nanostructures

Stephan Schnez,* Johannes Güttinger, Magdalena Huefner, Christoph Stampfer,† Klaus Ensslin, and Thomas Ihn
Solid State Physics Laboratory, ETH Zürich, 8093 Zürich, Switzerland
(Received 31 August 2010; published 26 October 2010)

We present scanning-gate images of a single-layer graphene quantum dot which is coupled to source and drain via two constrictions. We image and locate conductance resonances of the quantum dot in the Coulomb-blockade regime as well as resonances of localized states in the constrictions in real space, which are interpreted in light of previous transport experiments. In addition our technique allows us to estimate the extent of these localized states, namely, radii of about 10–13 nm.

DOI: 10.1103/PhysRevB.82.165445 PACS number(s): 73.23.Hk, 73.63.Kv, 73.22.Pr

I. INTRODUCTION

Graphene has sparked intense research among theorists and experimentalists[1,2] alike since its first successful fabrication in 2004.[3] This is mainly due to graphene's extraordinary band structure, a linear relationship between energy and momentum without a band gap. The gapless band structure, however, prohibits confining charge carriers by using electrostatic gates. Hence, lateral confinement in graphene relies on etched structures and the appearance of a transport gap in graphene constrictions.[4–6] Nevertheless, already the first experiment on graphene nanoribbons by Han *et al.*[7] showed a discrepancy between the measured transport gap and a simple confinement-induced band gap. Theoretical models explain the observed gap by Coulomb blockade, edge scattering, and/or Anderson-type localization due to edge disorder.[8–11] On the experimental side, there is increasing evidence for Coulomb-blockade effects in nanoribbons.[6,12–16]

Transport through graphene quantum dots in the Coulomb-blockade regime is typically modulated by resonances arising from the constrictions.[17] However, for both, nanoribbons and quantum dots, the microscopic origin of the transport gap and the resonances in the constrictions needs to be understood in more detail.

Hence, probing techniques which are capable of locally investigating properties of graphene nanostructures are essential. Earlier experiments of this kind on graphene include experiments with a scanning single-electron transistor,[18,19] scanning-tunneling spectroscopy,[20–22] and scanning-gate microscopy.[23–26] All these experiments were performed on large-area graphene sheets. Here we present results of scanning-gate experiments on a single-layer graphene quantum dot which is coupled to source and drain leads via two constrictions. We observe ringlike resonances in the scanning-gate experiments centered at the quantum dot as well as in the constrictions. This exhibits similarities to a recently reported experiment where Coulomb islands in a quantum Hall interferometer could be imaged.[27] Scanning-gate microscopy therefore enables us to map resonances in real space.

II. MEASUREMENTS

A. Sample characteristics

The graphene sample has been fabricated by mechanical exfoliation of natural graphite and subsequent deposition on a highly doped silicon wafer covered by 285 nm of silicon dioxide. Raman spectroscopy confirmed that the flake consisted of a single atomic layer. A final e-beam step is used to pattern Ti/Au electrodes. A detailed description of the fabrication process is given in Ref. 5. Figure 1(a) shows an atomic-force micrograph of the quantum dot (QD) and nearby in-plane gates (left and right side gates, LG and RG, and plunger gate PG) under ambient conditions after etching and removing the protective resist layer. The quantum dot has a lithographic radius of $r \approx 110$ nm; the two constrictions have a width of 30–40 nm. The completed device shown in Fig. 1(b) was imaged at $T \approx 2.6$ K *in situ* with our home-built atomic-force microscope.[28] If not stated otherwise, the temperature of all measurements shown in this paper is $T=2.6$ K.

We first show a backgate sweep in Fig. 1(c) with voltage $V_{\mathrm{bias}}=500$ μV applied between source and drain. The current through the dot is suppressed in the transport gap ranging approximately from 15 to 45 V. The charge-neutrality point is at $V_{\mathrm{BG}} \approx 30$ V, presumably because of charged impurities on or near the graphene surfaces. The charge-stability diagram of the quantum dot in 1(d) was measured at the base temperature $T=90$ mK of the dilution refrigerator. We extract a charging energy $\Delta E_C=3.5$ meV which is comparable to the values found in other devices of similar size.[5]

B. Scanning-gate measurements

We performed scanning-gate measurements of the quantum dot in the hole regime at $V_{\mathrm{BG}}=12$ V. To this end, we equipped an Oxford Instruments Kelvinox 100 dilution refrigerator with a home-built AFM.[28] In order to obtain a scanning-gate image, the AFM feedback is turned off and a constant voltage V_{tip} is applied to the tip. The conductance G_{dot} through the dot is then recorded as a function of tip position while scanning the tip at constant height above the sample.[29–31] Coulomb resonances of the quantum dot occur whenever the tip-induced potential shifts an energy level of the quantum dot into resonance with the electrochemical potential of source and drain. Hence, the rings can be regarded as contour lines of constant electrochemical potential in the dot.[31] The energy difference of neighboring contour lines is ΔE_C, the charging energy of the dot. The contour line pattern reflects the tip-induced potential as sensed by the quantum-dot states. If there are—apart from the designated quantum

 ©2010 The American Physical Society

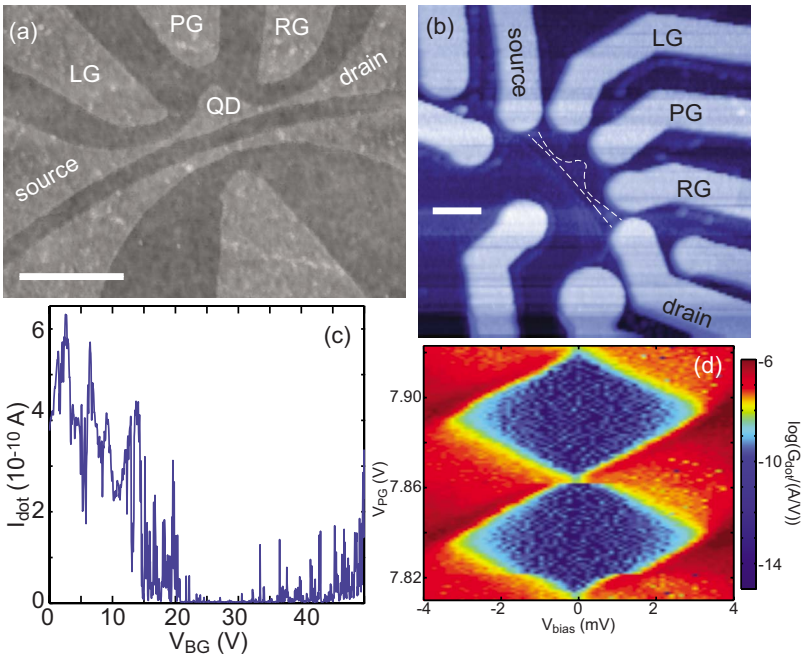

FIG. 1. (Color online) (a) Atomic force micrograph of the graphene sample after reactive ion etching obtained under ambient conditions. The QD is connected to source and drain via two constrictions. The nearby nanoribbon can be used as a charge detector but it was not connected in the measurements presented here. (b) *In situ* atomic force micrograph of the sample after cooldown at $T \approx 2.6$ K. This image was taken after positioning the tip above the sample with our home-built AFM (Ref. 28). The scale bar in (a) denotes 500 nm, in (b) 1 μm. (c) Backgate trace taken at $T \approx 2.6$ K and $V_{bias} = 500$ μV. The charge neutrality point is shifted to $V_{BG} \approx 30$ V. (d) Charge-stability diagram of the quantum dot. The charging energy is found to be $\Delta E_C = 3.5$ meV at $V_{BG} = 15$ V and $T = 90$ mK. The speckling inside the diamonds is due to calculating the derivative $G_{dot} = \partial I_{dot} / \partial V_{bias}$ numerically.

dot—additional localized states, a scanning-gate image will reflect their existence by additional sets of rings centered at the location of the states. These rings will cross the Coulomb resonances of the quantum dot at specific points in space. We will analyze the appearance of additional sets of rings in our graphene quantum dot below.

A representative result is shown in Fig. 2. The scan frame has an area of 1.4×1.4 μm^2 and the outline of the quantum dot, as obtained from topographical images [see Fig. 1(b)], is shown with dashed, black lines. We observe three sets of concentric rings which are marked by arrows labeled (QD), (A), and (B). The set (QD) is caused by Coulomb resonances of the quantum dot as verified by the presence of Coulomb-blockade diamonds when sweeping the tip and bias voltages (not shown here) and we refer to them as *Coulomb rings*. The conductance G_{dot} does not drop to zero between two Coulomb rings because the measurements were done at the edge of the transport gap in backgate voltage where the coupling of dot states to source and drain is rather strong.

Most strikingly, we observe two additional sets of rings (A) and (B). In the following, we will refer to them as *resonances* A and B, respectively. In all scanning-gate images taken on this sample, resonances A and B are manifest as amplitude modulations of the Coulomb resonances of the quantum dot. They are centered around points in the constrictions connecting the quantum dot to source and drain. Their presence allows to locate regions of localized charge carriers in the constrictions. This is a central result of this paper. The interpretation of rings A and B as being due to *localized states* will be corroborated below. Only one localized state is observed in each constriction.

In electronic transport, resonances are, in general, localized in space and sharp in energy. In order to confirm this for resonances A and B, we took linescans between points P and Q in Fig. 2 and changed the energy of the localized states by stepping the left-side gate voltage V_{LG} from 5 V up to 10 V. The result is shown in Fig. 3(a). We can identify quantum-

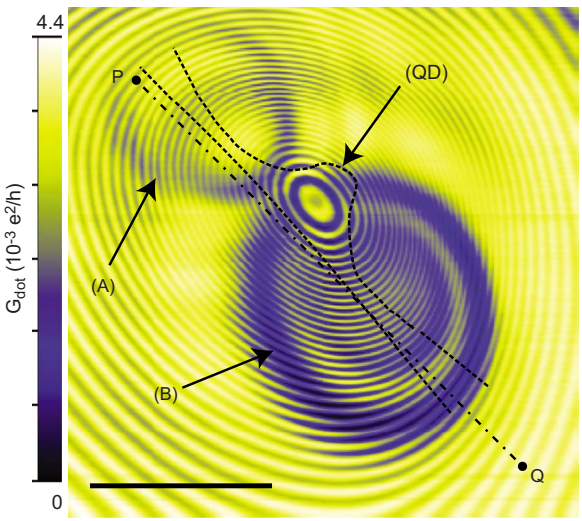

FIG. 2. (Color online) Scanning-gate image in the hole regime, $V_{BG} = 12$ V. The tip voltage was $V_{tip} = 2$ V, left gate voltage $V_{LG} = 0.15$ V, and the scan frame has a size of 1.4×1.4 μm^2. A symmetric bias of $V_{bias} = 300$ μV was applied across source and drain and the tip was scanned at a constant height of $\Delta z \approx 120$ nm above the sample. Coulomb resonances of the quantum dot show up as concentric rings denoted by arrow (QD). The center of the Coulomb resonances is offset from the topographic center of the dot by approximately 240 nm. Such a behavior, known from previous scanning-gate experiments, is of minor importance here (Ref. 31). The outline of the quantum dot and its connection to source and drain via the two constrictions, depicted with dashed, black lines, is corrected for the offset, assuming that the Coulomb resonances are centered in the quantum dot. Most striking, however, is the appearance of two more sets of concentric rings which are highlighted by arrows (A) and (B) and which are centered around points in the constrictions. The black, dashed-dotted line between points P and Q denotes the line along which the linescan of Fig. 3 was taken. The scale bar denotes 500 nm.

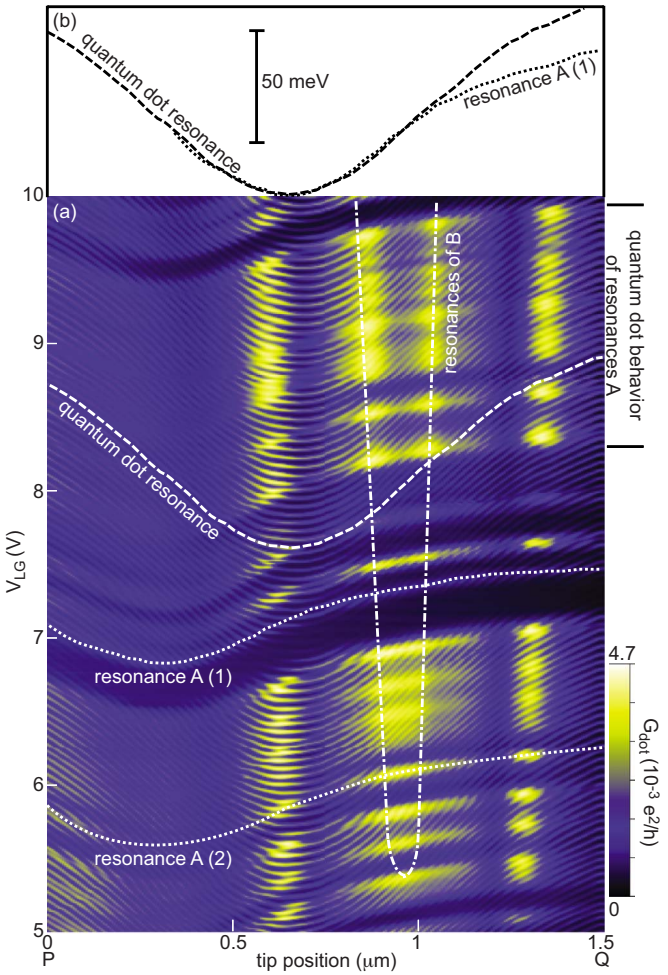

FIG. 3. (Color online) (a) Linescans along the dashed-dotted line between points P and Q depicted in Fig. 2 while the left gate was stepped from 5 to 10 V. The other parameters are the same as in Fig. 2. We can clearly distinguish between features of resonances A and B and the quantum dot. Two resonances of A are highlighted with white, dotted lines labeled (1) and (2), a quantum-dot resonance is highlighted with a white, dashed line, and a resonance of B is denoted with a white, dashed-dotted line. The upper, broad resonance (1) of A does not show any charging effect, whereas the lower, sharp one (2) is accompanied with avoided crossings of the Coulomb resonances. (b) Shifting resonance (1) of A along the x axis and scaling it by 1.67 lead to the determination of relative lever arms between quantum dot and resonance A as explained in the text.

dot resonances (dashed, white line and resonances parallel to it), resonances A (dotted, white lines and resonances parallel to them), and resonances B (dashed-dotted line and resonance parallel to it).

The tip-induced potential at any fixed location in the graphene plane is changed when moving the tip from P to Q. We stay on a particular resonance by compensating for this change at the location of the resonance with V_{LG}. This leads to the characteristic slopes of resonances A and B and the quantum-dot resonances. The left side gate is closest to the center of resonance A; resonance B is furthest away. Therefore resonances A are strongly tuned by the left gate whereas resonances B are only slightly affected. Quantum-dot resonances are in between. Below we will use this effect to deduce the lever arm ratio $\alpha_{LG}^{loc}/\alpha_{LG}^{dot}$ of the lever arms of the left gate on the dot, α_{LG}^{dot}, and on resonance A, α_{LG}^{loc}.

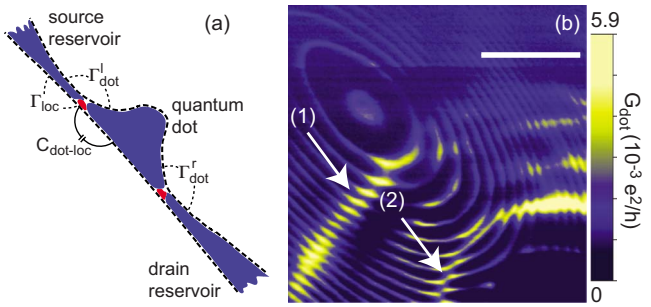

FIG. 4. (Color online) (a) Model for explaining the essential features induced by localized states in the constrictions. For simplicity, we consider just one localized state (upper red puddle next to the source lead) which is coupled to the source lead via the tunnel coupling Γ_{loc}. $C_{dot\text{-}loc}$ denotes the capacitive coupling between the localized state and the quantum dot. (b) Scanning-gate measurements at $T \approx 90$ mK measured at the mixing chamber. The image was taken at $V_{BG}=12$ V, $V_{bias}=35$ μV, $V_{tip}=-100$ mV, and a tip height of $\Delta z=40-45$ nm; the scan frame covers an area of 0.3×0.3 μm^2. Compared to 2, Coulomb resonances are much sharper due to the lower temperature. Although this measurement and 2 and 3 were taken at the same backgate voltages, a direct comparison of them is difficult because of several charge rearrangements in between. The crossings of Coulomb resonances and resonances of B lead to a modulation of G_{dot} and no avoided crossing of Coulomb resonance for arrow (1) and to avoided crossings for arrow (2). The scale bar denotes 100 nm.

Horizontal cuts in Fig. 3(a), i.e., cuts for fixed V_{LG}, show that all resonances eventually shrink to a single point in space. This allows us to identify them with states localized in space at this point. Vertical cuts, on the other hand, show that they are reasonably sharp in energy. However, we notice a strong variation in the width of the resonances; e.g., resonance A(2) is much sharper than resonance A(1). A closer inspection of the sharper resonances of A reveals that they are accompanied with avoided crossings of the quantum-dot Coulomb resonances.

III. INTERPRETATION

We propose the model shown in Fig. 4(a) which is capable of capturing the essential details of our observations. It consists of a quantum dot coupled to source and drain via two tunnel barriers with tunnel coupling $\Gamma_{dot}^{l,r}$. We introduce an additional localized state located in the constriction and coupled to the lead via a tunnel barrier with coupling Γ_{loc}. The localized state interacts with the quantum-dot states by tunneling through the barrier and by mutual capacitive coupling via $C_{dot\text{-}loc}$.

Figure 4(b) shows a scanning-gate image taken at the temperature $T \approx 90$ mK. Coulomb resonances are now much sharper than in Figs. 2 and 3(a). Resonances B lead to a modulation of the dot conductance G_{dot} as highlighted by arrows (1) and (2). The capacitive coupling between resonance B and the quantum dot leads to the avoided crossings

pointed at by arrow (2). They are more easily identified compared to Fig. 3(a) because of the lower temperature.

Whenever such an avoided crossing occurs, resonance A or B is charged with an additional charge carrier. Thus resonances originate from localized states. The capacitive coupling $C_{\text{dot-loc}}$ shifts the chemical potential in the dot when the localized state is charged. Consequently, the Coulomb ring in the scanning-gate image is shifted as well. Charging effects are not observed for all crossings of quantum-dot resonances with resonances A or B. Avoided crossings of Coulomb resonances occur only for narrow resonances A and B; the broader ones do not show the signature of charge quantization as inspection of Figs. 3 and 4 show. The tunnel coupling strength Γ_{loc} must therefore depend strongly on the Fermi energy. Then charging of a localized state with discrete charges occurs only if Γ_{loc} is below a certain threshold such that the condition $G_{\text{loc}}(\Gamma_{\text{loc}}) < e^2/h$ for the conductance of the localized state is fulfilled. The width of the resonance is also determined by the tunnel coupling if $\Gamma_{\text{loc}} > 4k_BT$.

Whenever a localized state shows quantum-dotlike behavior, we can infer its size from its charging energy. In order to do so, we pick just those resonances of A in Fig. 3 which show avoided crossings with quantum-dot resonances. We identify six resonances of this type in the regime denoted by "quantum-dot behavior of resonances A." They have a spacing of $\Delta V_{\text{LG}}^{\text{loc}} \approx 270-370$ mV in left-gate voltage. In order to convert this voltage scale to an energy, we need to know the lever arm $\alpha_{\text{LG}}^{\text{loc}}$ of the left gate onto the localized state. The desired lever arm is obtained from Fig. 3 by comparing resonances of the quantum dot with resonances of the localized state.

Coulomb resonances of the quantum dot are separated on average by $\Delta V_{\text{LG}}^{\text{dot}} = 53$ mV in left-gate voltage. Combined with the charging energy $\Delta E_C = 3.5$ meV, this yields a lever arm of $\alpha_{\text{LG}}^{\text{dot}} = 0.066$. The two dotted lines in Fig. 3(a) denote how resonances of A evolve as a function of position. If we scale these lines by a factor of 1.67 in V_{LG} direction and shift them along the x axis (the "position") such that their minima coincide with a minimum of a Coulomb resonance, they nicely fit onto each other as shown in Fig. 3(b).[32] The desired lever arm $\alpha_{\text{LG}}^{\text{loc}}$ is given by $\alpha_{\text{LG}}^{\text{loc}} = \alpha_{\text{LG}}^{\text{dot}} \cdot 1.67 = 0.110$.

Consequently the charging energy $\Delta E_C^{\text{loc}} = \alpha_{\text{LG}}^{\text{loc}} \cdot e\Delta V_{\text{LG}}^{\text{loc}}$ of the localized state A is between 30 and 41 meV. This corresponds to a radius of the localized state of $r_{\text{loc}} = 10-13$ nm assuming $\Delta E_C^{\text{loc}}/\Delta E_C = r/r_{\text{loc}}$ with $\Delta E_C = 3.5$ meV and lithographic size of the dot $r = 110$ nm. Previous experiments obtained similar sizes by means of conventional transport experiments for graphene nanoribbons.[12,13,33] However, our method allows us to determine relative lever arms of localized states in more complex structures such as the presented quantum-dot device.

Stampfer *et al.*[14] reported on a variation in relative lever arms of localized states in nanoribbons by up to 30%. This was explained with a number of localized states spread along the nanoribbon. Based on the geometry of the device used in Ref. 14, a rough estimate yields a typical separation between localized states of more than 300 nm. With our scanning-gate microscope, a separation of more than 100 nm should be easily detectable. In our measurements on the quantum dot in the hole regime, we typically observed one localized state per constriction at $T = 2.6$ K and for a range of Fermi energies. In some rare cases, we found indications of more than one resonance in a single constriction separated on a scale of ~ 100 nm. We speculate that the observation of one localized state per constriction at a given Fermi energy and at $T = 2.6$ K is due to the short length of the constriction.

In Fig. 2 we can distinguish more than 30 Coulomb rings with a spacing of around 20 nm for some pairs of rings. This corresponds to an energy gradient $\Delta\epsilon_{\text{res}} = \Delta E_C/20$ nm ≈ 0.2 meV/nm. We define the spatial resolution Δx_{res} as the minimal separation of two localized states which we can resolve with the scanning-gate tip. It is limited by the width Γ_{res} of the resonances. We estimate the spatial resolution from $\Delta x_{\text{res}} = \Gamma_{\text{res}}/\Delta\epsilon_{\text{res}}$.[34] The best resolution is obtained for thermally broadened resonances, $\Gamma_{\text{res}} \approx 4k_BT$, yielding $\Delta x_{\text{res}} \approx 5$ nm for $T = 2.6$ K. However, if the resonance is tunnel-coupling broadened by, e.g., a factor of ten compared to temperature, the spatial resolution decreases to $\Delta x_{\text{res}} \approx 50$ nm. In that case, the potential existence of two localized sites within the constriction could not be resolved with our scanning-gate microscope.

IV. CONCLUSION

In conclusion, we performed scanning-gate microscopy on a graphene quantum dot. We imaged and located resonant states of the quantum dot and the constrictions in real space. The gate-voltage dependence of resonances related to localized states is in full agreement with previous transport studies. Our measurements add local information suggesting that one (or few) localized sites exist in the small constrictions within an area of $\sim 40 \times 40$ nm^2, which strongly influence the coupling of the quantum dot to the leads. Moreover we could also estimate charging energies and corresponding sizes of the localized states to be 30–41 meV and 10–13 nm, respectively.

ACKNOWLEDGMENTS

Financial support by ETH Zürich and the Swiss National Science Foundation is gratefully acknowledged. Some images have been prepared using the WSXM-software (Ref. 35).

*schnez@phys.ethz.ch

†Present address: JARA-FIT and II. Institute of Physics, RWTH Aachen, 52074 Aachen, Germany.

[1] A. K. Geim and K. S. Novoselov, Nature Mater. **6**, 183 (2007).

[2] A. H. Castro Neto, F. Guinea, N. M. R. Peres, K. S. Novoselov, and A. K. Geim, Rev. Mod. Phys. **81**, 109 (2009).

[3] K. S. Novoselov, A. K. Geim, S. V. Morozov, D. Jiang, M. I. Katsnelson, S. V. Dubonos, I. V. Grigorieva, and A. A. Firsov,

Science **306**, 666 (2004).
[4] L. A. Ponomarenko, F. Schedin, M. I. Katsnelson, R. Yang, E. W. Hill, K. S. Novoselov, and A. K. Geim, Science **320**, 356 (2008).
[5] C. Stampfer, J. Güttinger, F. Molitor, D. Graf, T. Ihn, and K. Ensslin, Appl. Phys. Lett. **92**, 012102 (2008).
[6] X. Liu, J. B. Oostinga, A. F. Morpurgo, and L. M. K. Vandersypen, Phys. Rev. B **80**, 121407(R) (2009).
[7] M. Y. Han, B. Özyilmaz, Y. Zhang, and P. Kim, Phys. Rev. Lett. **98**, 206805 (2007).
[8] F. Sols, F. Guinea, and A. H. Castro Neto, Phys. Rev. Lett. **99**, 166803 (2007).
[9] E. R. Mucciolo, A. H. Castro Neto, and C. H. Lewenkopf, Phys. Rev. B **79**, 075407 (2009).
[10] M. Evaldsson, I. V. Zozoulenko, H. Xu, and T. Heinzel, Phys. Rev. B **78**, 161407(R) (2008).
[11] G. Schubert, J. Schleede, and H. Fehske, Phys. Rev. B **79**, 235116 (2009).
[12] K. Todd, H.-T. Chou, S. Amasha, and D. Goldhaber-Gordon, Nano Lett. **9**, 416 (2009).
[13] F. Molitor, A. Jacobsen, C. Stampfer, J. Güttinger, T. Ihn, and K. Ensslin, Phys. Rev. B **79**, 075426 (2009).
[14] C. Stampfer, J. Güttinger, S. Hellmüller, F. Molitor, K. Ensslin, and T. Ihn, Phys. Rev. Lett. **102**, 056403 (2009).
[15] P. Gallagher, K. Todd, and D. Goldhaber-Gordon, Phys. Rev. B **81**, 115409 (2010).
[16] J. B. Oostinga, B. Sacépé, M. F. Craciun, and A. F. Morpurgo, Phys. Rev. B **81**, 193408 (2010).
[17] C. Stampfer, E. Schurtenberger, F. Molitor, J. Güttinger, T. Ihn, and K. Ensslin, Nano Lett. **8**, 2378 (2008).
[18] J. Martin, N. Akermann, G. Ulbricht, T. Lohmann, J. H. Smet, K. von Klitzing, and A. Yacoby, Nat. Phys. **4**, 144 (2008).
[19] J. Martin, N. Akermann, G. Ulbricht, T. Lohmann, K. von Klitzing, J. H. Smet, and A. Yacoby, Nat. Phys. **5**, 669 (2009).
[20] Y. Zhang, V. W. Brar, F. Wang, C. Girit, Y. Yayon, M. Panlasigui, A. Zettl, and M. F. Crommie, Nat. Phys. **4**, 627 (2008).
[21] Y. Zhang, V. W. Brar, C. Girit, A. Zettl, and M. F. Crommie, Nat. Phys. **5**, 722 (2009).
[22] G. Li, A. Luican, and E. Y. Andrei, Phys. Rev. Lett. **102**, 176804 (2009).
[23] J. Berezovsky, M. F. Borunda, E. J. Heller, and R. M. Westervelt, Nanotechnology **21**, 274013 (2010).
[24] J. Berezovsky and R. M. Westervelt, Nanotechnology **21**, 274014 (2010).
[25] M. R. Connolly, K. L. Chiou, C. G. Smith, D. Anderson, G. A. C. Jones, A. Lombardo, A. Fasoli, and A. C. Ferrari, Appl. Phys. Lett. **96**, 113501 (2010).
[26] R. Jalilian, L. Jauregui, G. Lopez, J. Tian, C. Roecker, M. Yazdanpanah, R. Cohn, I. Jovanovic, and Y. Chen, arXiv:1003.5404 (unpublished).
[27] B. Hackens, F. Martins, S. Faniel, C. A. Dutu, H. Sellier, S. Huant, M. Pala, L. Desplanque, X. Wallart, and V. Bayot, Nat. Commun. **1**, 39 (2010).
[28] A. E. Gildemeister, T. Ihn, C. Barengo, P. Studerus, and K. Ensslin, Rev. Sci. Instrum. **78**, 013704 (2007).
[29] M. A. Topinka, B. J. LeRoy, R. M. Westervelt, S. E. J. Shaw, R. Fleischmann, E. J. Heller, K. D. Maranowski, and A. C. Gossard, Nature (London) **410**, 183 (2001).
[30] A. Pioda, S. Kicin, T. Ihn, M. Sigrist, A. Fuhrer, K. Ensslin, A. Weichselbaum, S. E. Ulloa, M. Reinwald, and W. Wegscheider, Phys. Rev. Lett. **93**, 216801 (2004).
[31] A. E. Gildemeister, T. Ihn, M. Sigrist, K. Ensslin, D. C. Driscoll, and A. C. Gossard, Phys. Rev. B **75**, 195338 (2007).
[32] For tip positions >1.1 μm, screening effects lead to a different progression of the quantum-dot resonance and the resonances of localized state A.
[33] M. Y. Han, J. C. Brant, and P. Kim, Phys. Rev. Lett. **104**, 056801 (2010).
[34] This expression holds if the typical width of the wave function in a localized state is small compared to the characteristic length over which the tip-induced potential rises. This is true here, given our experimental results.
[35] I. Horcas, R. Fernandez, J. M. Gomez-Rodriguez, J. Colchero, J. Gomez-Herrero, and A. M. Baro, Rev. Sci. Instrum. **78**, 013705 (2007).